Cell Reports

Article

A *Plasmodium falciparum* lysophospholipase regulates host fatty acid flux via parasite lipid storage to enable controlled asexual schizogony

Graphical abstract

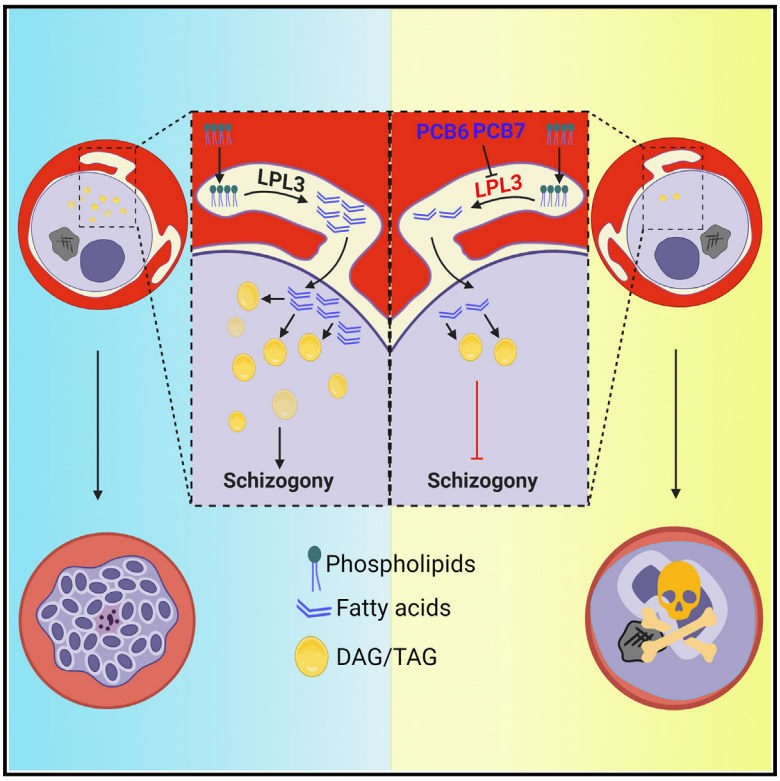

Authors

Pradeep Kumar Sheokand, Yoshiki Yamaryo-Botté, Monika Narwal, ..., Mohd Asad, Cyrille Y. Botté, Asif Mohmmed

Correspondence

cyrille.botte@univ-grenoble-alpes.fr (C.Y.B.), amohd@icgeb.res.in (A.M.)

In brief

Lipid acquisition is essential for malaria parasite survival. Sheokand et al. show that the parasite uses a lysophospholipase (LPL3) at the host-parasite interface to generate fatty acids from host lipids that are stored and timely mobilized to allow parasite division. The authors identify specific LPL3 inhibitors that kill the parasite.

Highlights

- *Pf*LPL3 is a critical lysophospholipase at host-parasite interface
- *Pf*LPL3 generates FAs from host lipids
- The FAs are stored as TAGs and timely mobilized to allow proper schizogony
- *Pf*LPL3 can be blocked by MMV compounds PCB6/7, killing parasite blood stages

Sheokand et al., 2023, Cell Reports *42*, 112251
April 25, 2023
https://doi.org/10.1016/j.celrep.2023.112251

CellPress

Cell Reports

CellPress
OPEN ACCESS

Article

A *Plasmodium falciparum* lysophospholipase regulates host fatty acid flux via parasite lipid storage to enable controlled asexual schizogony

Pradeep Kumar Sheokand,[1] Yoshiki Yamaryo-Botté,[2] Monika Narwal,[1] Christophe-Sébastien Arnold,[2] Vandana Thakur,[1] Md Muzahidul Islam,[1] Mudassir M. Banday,[1] Mohd Asad,[1] Cyrille Y. Botté,[2,3,4,*] and Asif Mohmmed[1,3,*]

[1]International Centre for Genetic Engineering and Biotechnology, New Delhi 110 067, India
[2]ApicoLipid Team, Institute for Advanced Biosciences, CNRS UMR5309, Université Grenoble Alpes, INSERM U1209, Grenoble, France
[3]These authors contributed equally
[4]Lead contact
*Correspondence: cyrille.botte@univ-grenoble-alpes.fr (C.Y.B.), amohd@icgeb.res.in (A.M.)
https://doi.org/10.1016/j.celrep.2023.112251

SUMMARY

Phospholipid metabolism is crucial for membrane biogenesis and homeostasis of *Plasmodium falciparum*. To generate such phospholipids, the parasite extensively scavenges, recycles, and reassembles host lipids. *P. falciparum* possesses an unusually large number of lysophospholipases, whose roles and importance remain to be elucidated. Here, we functionally characterize one *P. falciparum* lysophospholipase, *Pf*LPL3, to reveal its key role in parasite propagation during asexual blood stages. *Pf*LPL3 displays a dynamic localization throughout asexual stages, mainly localizing in the host-parasite interface. Inducible knockdown of *Pf*LPL3 disrupts parasite development from trophozoites to schizont, inducing a drastic reduction in merozoite progenies. Detailed lipidomic analyses show that *Pf*LPL3 generates fatty acids from scavenged host lipids to generate neutral lipids. These are then timely mobilized to allow schizogony and merozoite formation. We then identify inhibitors of *Pf*LPL3 from Medicine for Malaria Venture (MMV) with potent antimalarial activity, which could also serve as pertinent chemical tools to study parasite lipid synthesis.

INTRODUCTION

Malaria is a vector-transmitted parasitic disease that remains a major medical problem in tropical and subtropical areas of the world. Malaria leads to ~500,000 to 1 million deaths globally every year.[1] In the absence of an efficient vaccine and because of the rapid spread of drug-resistant parasite strains, there is an urgent need to identify new drug targets and to develop new drugs against the disease. Understanding key metabolic pathways in the parasite, which are essential for parasite survival, is a crucial pre-requisite to identify unique and potent targets in the parasites. The pathological symptoms of malaria are caused by repeated blood-stage asexual cycles of the parasite in host erythrocytes. Different parasite development stages during the asexual life cycle involve extensive coordinated lipid synthesis, modification of host cell membrane, and biogenesis membrane needed for parasite division and propagation.[2] This high demand of lipids/phospholipids (PLs) required for extensive membrane synthesis is fulfilled by scavenging from the host milieu, recycling and modifying host lipids, *de novo* synthesis, and re-shuffling of those through parasite lipid synthesis machinery.[3,4] The high demand for lipids by the parasite is perfectly illustrated in *P. falciparum* asexual blood stages, where lipid content increases by 200%–300% through the acquisition and synthesis of a large number of lipid species for growth and proliferation.[4,5]

PLs are the major structural components of parasite membranes and are used to make new daughter cells. Phosphatidylcholine (PC) is the most abundant PL in *Plasmodium* membranes during both liver stages and blood stages, attesting to its importance for parasite division and propagation.[4,6] The parasite possesses the typical eukaryotic *de novo* PL synthesis machinery to generate most (lyso)phospholipids classes and their precursors from fatty acids (FAs) and polar heads, i.e., the so-called Kennedy pathway and the cytidine diphosphate-diacylglycerol (CDP-DAG) pathway. *P. falciparum* blood stages notably rely on the scavenging of lysophosphatidylcholine (LPC), especially its polar head phosphocholine, to fuel this *de novo* synthesis of PC and maintain high asexual division rates.[7,8] The absence of LPC in the extracellular media drives parasite sexual differentiation into gametocytes, likely by the lack of PC used as a building material for active asexual division. Because LPC plays an important role in parasite development and differentiation, enzymes involved in its hydrolysis are considered attractive targets for antimalarial development. Importantly, it was shown that the related apicomplexan, *T. gondii*, massively scavenges host FAs generated from host PL, and that the parasite needs to channel this otherwise toxic flux of FA toward lipid storage (i.e., lipid droplets) in the form of triacylglycerols (TAGs) for a controlled utilization.[9] *P. falciparum* also depends on massive host lipid scavenging, but very little is known about how the

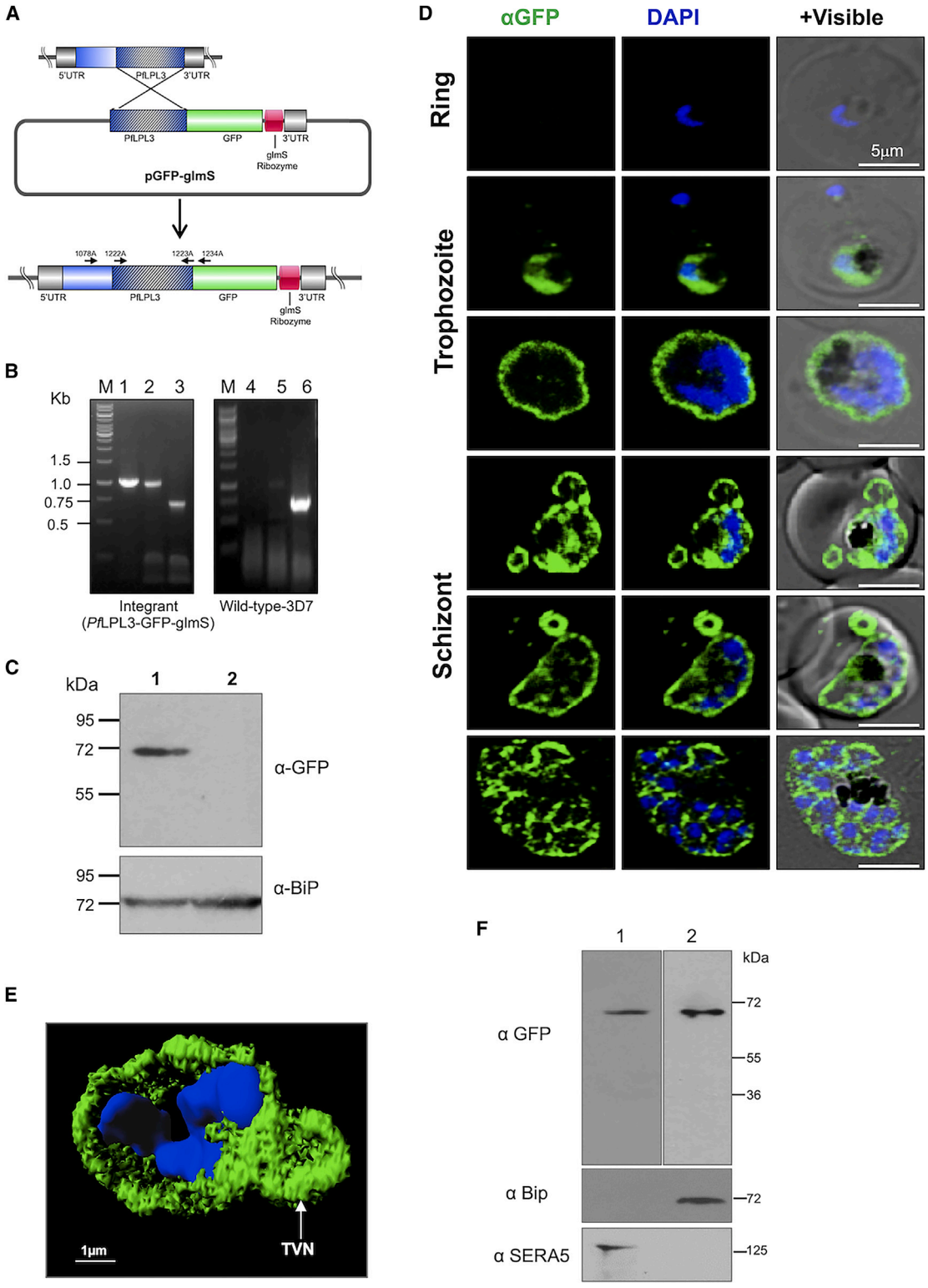

Figure 1. Generation of *Pf*LPL3-GFP-*glm*S transgenic parasite line

(A) A schematic representation of single crossover homologous recombination showing the integration of the LPL3-GFP-*glm*S plasmid at the C terminus of the endogenous *pflpl3* gene.

(legend continued on next page)

parasite generates and uses scavenged FA. The catabolism of lipid metabolites from the host must therefore involve phospholipases to manipulate the scavenged lipids and generate the proper precursors (i.e., FAs and polar heads). Indeed, the parasite contains a high number of phospholipases, harboring α/β hydrolase domain, including a family of lysophospholipases (LPLs). The LPLs play key roles in recycling lipids by hydrolysis of acyl chains from lysophospholipids, which are the intermediates in the metabolism of membrane phospholipids.

In the present study, we have functionally characterized one of the *P. falciparum* LPLs (*Pf*LPLs), *Pf*LPL3 (PlasmoDB Gene ID: PF3D7_1476800), which is essential for blood-stage schizogonic division through recycling of host lipids. We used a GFP-*glm*S ribozyme approach,[10] which allowed the endogenous localization of the protein, as well as inducible-transient downregulation during the parasite blood stages. Confocal analyses showed that *Pf*LPL3 has a dynamic localization at interfaces between the parasite and the host cell, at the parasitophorous vacuole (PV), and extending into the tubulovesicular network (TVN) space within the host erythrocytes, more specifically during late-trophozoite and schizont stages. Transient knockdown of *Pf*LPL3 caused dramatic hindrance in schizont development, as well as a significant decrease in the number of merozoite progenies generated in each schizont. To determine the function of *Pf*LPL3 for merozoite formation and parasite survival, we performed comprehensive lipidomic analyses, which showed that disruption of *Pf*LPL3 induced drastic changes in parasite lipid composition and homeostasis, impacting FAs, PLs, and neutral lipid contents. Specifically, lipidomic analyses revealed that *Pf*LPL3 generates free FAs (FFAs) that normally fuel the DAG-TAG synthesis pathway for lipid storage. This, in turn, regulates the active synthesis of PLs, which are essentially required for membrane biogenesis of merozoites during schizogony. We developed an *in vitro* activity assay using recombinant *Pf*LPL3 that confirmed LPL activity for the enzyme. Using this activity assay, we screened the existing Medicine for Malaria Venture (MMV) ''Malaria Box'' compounds chemo library. We were able to identify two specific inhibitors of *Pf*LPL3 enzymatic activities with potent parasitical efficacies ($\sim$1.0 μM range). Importantly, treatment of blood-stage parasites phenocopied the disruption of *Pf*LPL3 in the parasite, confirming their selectivity for *Pf*LPL3. Based on the importance of *Pf*LPL3 for blood-stage parasite development, these compounds could be further developed as antimalarials and/or chemical tools specifically targeting lipid homeostasis machinery in the malaria parasite.

RESULTS

Endogenous tagging of *pfLPL3* gene and localization of fusion protein in transgenic parasites

The *Pf*LPL3 protein (PlasmoDB Gene ID: PF3D7_1476800) contains the conserved active-site residues of LPL (Figure S1); the *Pf*LPL3 gets expressed in the asexual stages in the young (10–20 h postinvasion [hpi]) and mature stages of the parasites (32–48 hpi). To determine the localization and function of the putative LPL *Pf*LPL3 during *P. falciparum* asexual blood stages, we generated a transgenic parasite line using the GFP-*glm*S C-terminal tagging approach. We used the GFP-*glm*S ribozyme system[10] for C-terminal tagging of the native *pfLPL3* gene, so that the fusion protein gets expressed under the control of the native promoter (Figure 1A). This allowed to endogenously tag *Pf*LPL3 and hence reveal its physiological localization, as well as to study its functional role by conditional knockdown strategy. Integration of the tag at the C terminus of the gene was confirmed in the selected clonal parasite population using PCR-based analyses (Figure 1B). Expression of the fusion protein of $\sim$70 kDa as predicted was detected by western blot analysis using the anti-GFP antibody (Figure 1C). The band was not detected in the wild-type 3D7 parasites. These transgenic parasites, *Pf*LPL3_GFP_*glm*S, were studied to determine the physiological localization of the *Pf*LPL3-GFP fusion protein by fluorescence and confocal microscopy approaches. The chimeric protein was expressed throughout all stages of the asexual blood life cycle of the parasite (Figure 1D). In early development stages, ring and mid-trophozoite stages, GFP fluorescence was mainly observed in the cytosol. As parasites matured into late-trophozoite and schizonts stages, the GFP labeling was observed at the parasite periphery, in the PV region. Intriguingly, during the late-trophozoite stages, *Pf*LPL3 was also found to be present in the PV extensions forming a host-parasite interface structure within the host RBC cytosol: at the TVNs (Figures 1D and S2A). A 3D reconstruction of trophozoite-stage parasite images clearly confirmed the presence of GFP staining around the parasite periphery and in the TVN (Figure 1E). To find out whether the *Pf*LPL3 was present outside the parasite plasma membrane, we fractionated infected RBCs from transgenic parasite culture by saponin lysis. *Pf*LPL3 was detected in the supernatant and in the pellet fraction by western blot analysis, which confirmed the presence of *Pf*LPL3 in the PV and in the parasite cytosol (Figure 1F), correlating with the fluorescence microscopy results. Further, we also confirmed the localization of the native *Pf*LPL3 in the

(B) PCR-based analyses of the selected clonal parasite culture and wild-type 3D7 parasite lines; locations of primers used are marked in the schematic. Lanes 1 and 4 (primers 1078A and 1234A) show amplification only in the integrants; lanes 2 and 5 (primers 1222A and 1234A) show amplification in integrants or episome parasites; lanes 3 and 6 (primers 1222A and 1223A) show amplification in both integrants and the wild-type line.

(C) Western blot of transgenic parasites probed with anti-GFP antibody. The fusion protein band was detected in the transgenic parasites, *Pf*LPL3-GFP-*glm*S only (lane 1) and not in the 3D7 parent parasite (lane 2). Blot was run in parallel and probed with anti-BiP (ER protein marker) was used as loading control.

(D) Fluorescent microscopic images of transgenic parasites showing localization of GFP-fusion protein at ring, trophozoite, and schizont stages. The parasite nuclei were stained with DAPI, and parasites were visualized by confocal laser scanning microscope. In young parasites, the fusion protein was observed in the cytosol of the parasite, but as the parasite matures, the fluorescence was observed toward the periphery of the parasite.

(E) The 3D image constructed by using series of z stack images of the transgenic parasites with IMARIS 7.0 shows the GFP-fusion protein present in the PV and tubulovesicular network (TVN) region.

(F) Western blot of infected erythrocytes fractions after saponin lysis showing that the *Pf*LPL3-GFP fusion protein is present in soluble fraction (lane 1) representing content of parasitophorous vacuole (PV) and host cytosol (lane 2); blot was run in parallel and probed with anti-BiP and anti-SERA5 (Serine Repeat Antigen protein5, speudoprotease of the PV) antibodies, which were used as negative and positive controls, respectively.

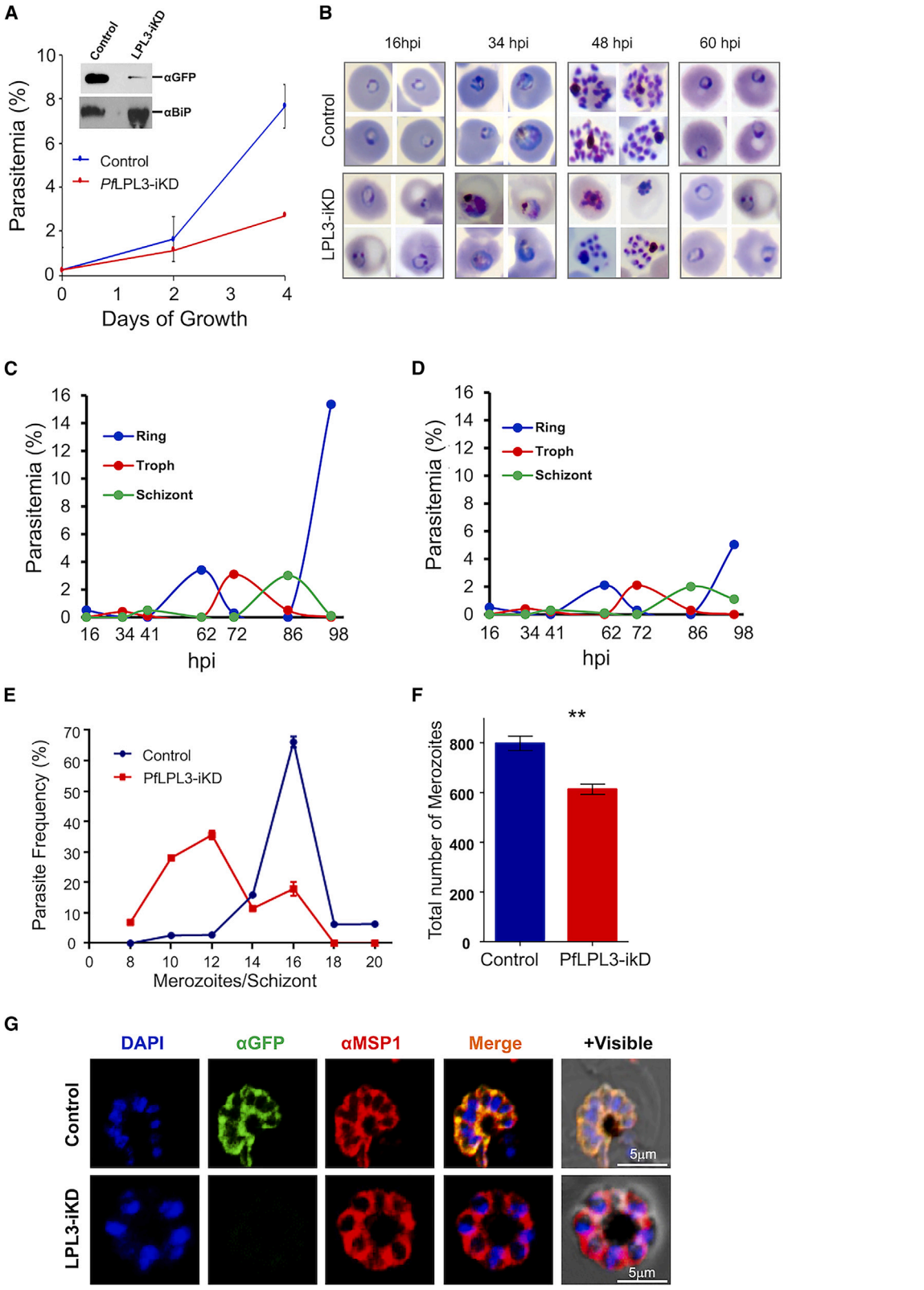

(legend on next page)

transgenic parasites by immuno-staining with anti-*Pf*LPL3 antibodies, which showed overlap labeling with that of the GFP-fusion protein (Figure S3).

To further investigate these localization patterns, we carried out membrane labeling and immuno-staining studies. The GFP-tagged parasites were co-stained with the lipid membrane probe BODIPY-TR ceramide (Bodipy-Cer), which can label any membranous structures. The Bodipy-Cer probe labeled the parasite periphery, including both plasma membrane and PV membrane (PVM) (Figure S2B). In addition, the Bodipy-Cer-labeled tubulovesicular extension of the PVM could also be observed in the erythrocyte cytosol for a section of the late-trophozoite/schizont-stage parasite population (Figure S2B). The *Pf*LPL3-GFP labeling showed overlap with BODIPY in the PV region and in the TVN (Figure S2B). Further, co-labeling of transgenic parasites with a PV-resident protein, SERA5,[11] confirmed the localization of *Pf*LPL3-GFP protein in the PV (Figure S2C).

Selective degradation of *Pf*LPL3 inhibits parasite growth

To understand the functional significance of *Pf*LPL3 and its possible involvement in lipid metabolism, we utilized the *Pf*LPL3_GFP_*glm*S parasite line for inducible knockdown of *Pf*LPL3 (*Pf*LPL3-iKD) expression using *glm*S ribozyme. In the presence of glucosamine (GlcN), the *glm*S-ribozyme cleaves itself, which in turn leads to degradation of the associated *Pf*LPL3 mRNA. Selective knockdown of *Pf*LPL3 protein was assessed in transgenic parasites treated with GlcN (1.25 mM). The parasites showed a reduction in *Pf*LPL3 levels (~90%) in treated sets (Figure 2A). To study the effect of the *Pf*LPL3-iKD on parasite growth, we determined total parasitemia at different time points (24, 36, and 48 h) after GlcN treatment. The *Pf*LPL3-iKD set showed ~70% inhibition of parasite growth compared with untreated parasites (Figures 2A and S4A). There was no deleterious effect of 2.5 mM GlcN on the growth of the wild-type parasite line (Figure S4B).

*Pf*LPL3 is important for parasite development and crucial for normal schizogonic division

To study the effect of selective degradation of *Pf*LPL3 on parasite development and morphology, we monitored the *Pf*LPL3-iKD set and control set after different time intervals (Figures 2B–2D and S4C–S4E). In the control set, during each intra-erythrocytic cycle, the parasites usually develop from ring to trophozoites to mature schizonts, and subsequent merozoites released from these schizonts can invade new erythrocytes. Morphological observations on parasite intracellular development showed no effect on the development of ring stages into trophozoite stages in *Pf*LPL3-iKD as compared with the control set (Figure 2B). However, aberrant development of late trophozoites and schizonts was observed in *Pf*LPL3-iKD, having smaller, aberrant, or sick-looking parasites compared with control (Figures 2B and S3A). A large number of trophozoites were not able to develop into schizonts, which caused ~50% reduction in the number of schizonts as compared with the control (Figures 2C and 2D). Indeed, at 48 hpi, a large number of stressed parasites were observed in the *Pf*LPL3-iKD set as compared with the control set (Figures 2B and S5A), which were not viable to develop into schizonts (Figures 2D and S5A). Further, the *Pf*LPL3-iKD parasites were more specifically affected at the replicative fitness of these schizonts. During schizogony, *P. falciparum* typically undergoes multiple rounds of nuclear divisions resulting in 16–32 merozoites. In the control set, the majority of the schizonts were found to contain 16 or more merozoites (Figure 2E). However, in the *Pf*LPL3-iKD parasite set, the mean number of merozoites per schizonts was significantly reduced (Figure 2E). This decrease in replicative fitness of schizonts resulted in an ~25% decrease in the total number of merozoites with respect to segmented schizonts (Figure 2F). It is to be pointed out that this effect is in addition to hampering of parasite development in the *Pf*LPL3-iKD set, and a large number of parasites were developmentally stuck even before the segmental stages. Therefore, only a few of the parasites could develop into segmented schizonts, which also harbored a reduced number of merozoites as compared with the control. However, immunostaining of these schizonts with anti-MSP1 antibody showed that there was no defect in the merozoites membrane in the *Pf*LPL3-iKD set, which suggested that the merozoite generated had a fully developed plasma membrane (Figures 2G and S5B). Overall, we show that *Pf*LPL3-iKD not only inhibited schizont development (>50%) but also reduced replicative fitness of parasites (~25%), which resulted in >70% parasite growth inhibition.

Downregulation of *Pf*LPL3 disrupts lipid homeostasis through decrease of neutral lipid content and concomitant increase of FFAs and PLs

To assess the role of *Pf*LPL3 for parasite membrane biogenesis, we conducted comprehensive mass spectrometry-based lipidomic analyses on total lipid extracted from the *Pf*LPL3-iKD set of parasites. Based on the predicted LPL function of *Pf*LPL3, i.e., releasing FA from existing (lyso)phospholipids, the total FA content of parasites was initially assessed. Logically, the disruption

Figure 2. Inducible knockdown of *Pf*LPL3 hampers parasite growth and survival

(A) Graph showing percentage parasitemia in *Pf*LPL3-GFP-*glm*S transgenic parasite cultures grown with 2.5 mM glucosamine (iKD) as compared with the parasites treated with solvent alone (control), as estimated by new ring-stage parasites after 2 and 4 days of growth. Error bars show standard deviation for each data point (n = 3). Western blot analysis showing reduction in the fusion protein in the presence of glucosamine is shown in inset; samples were treated with 2.5 mM glucosamine at ring stages (18–20 hpi) and harvested at late-trophozoite/schizont stages (36–40 hpi) for western blot analysis.

(B) Giemsa-stained images of parasites showing effect on parasite morphology at different time points (0–48 h) for control and *Pf*LPL3-iKD sets.

(C and D) Parasite-stage progression curve for (C) control and (D) *Pf*LPL3-iKD sets.

(E) Frequency distribution of number of merozoites per schizont at 48 hpi in the control and *Pf*LPL3-iKD parasite set.

(F) Graph showing reduction in the total number of merozoites in *Pf*LPL3-iKD parasite line in comparison with the control (n = 50 segmented schizonts). $^{**}p < 0.01$.

(G) Fluorescent images of control and *Pf*LPL3-iKD parasites immunostained with anti-MSP1 antibody suggesting that there is no defect in the merozoites membrane in the *Pf*LPL3-iKD set.

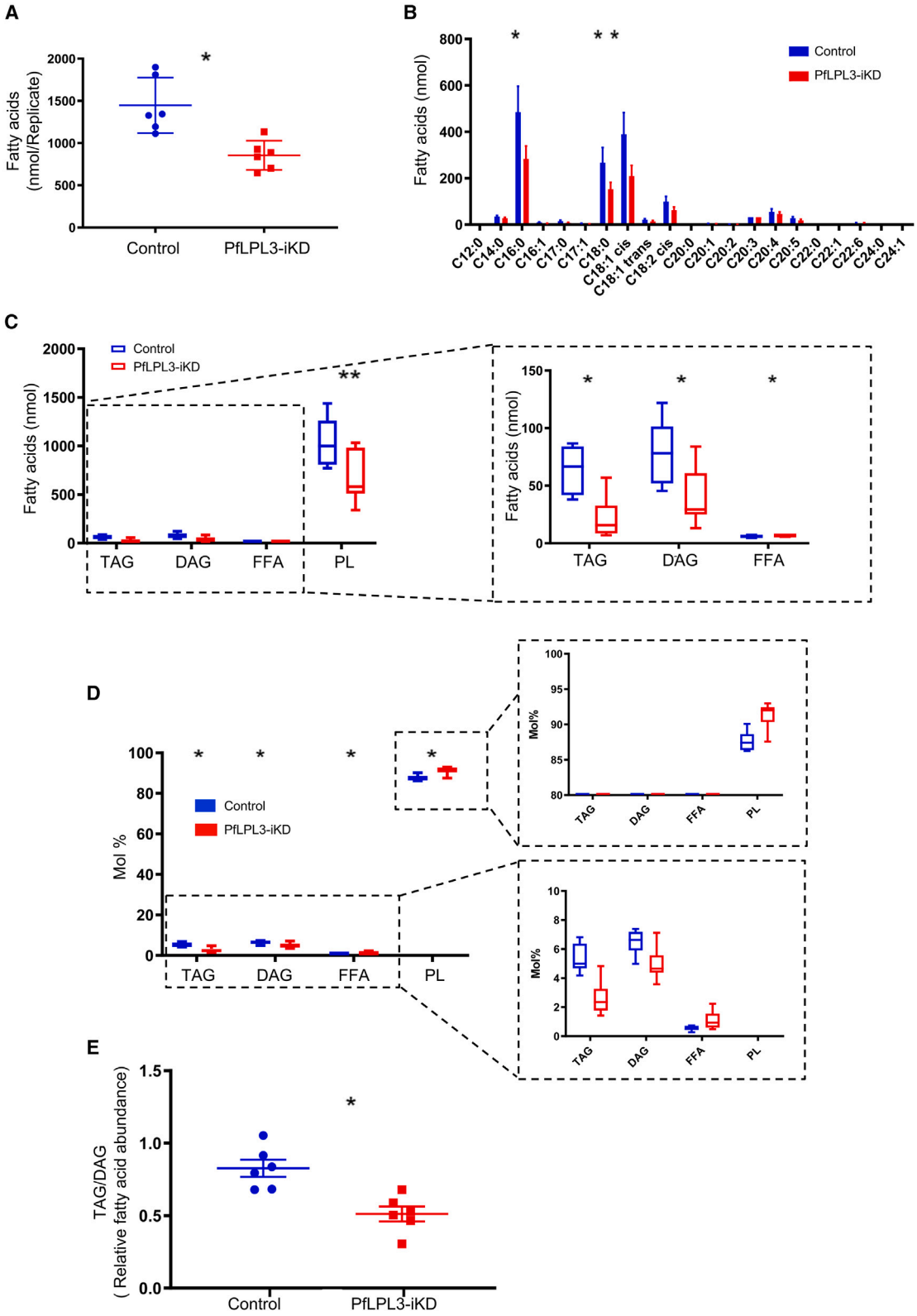

(legend on next page)

of *Pf*LPL3 induced a significant reduction of total FA abundance (in nmol) (Figure 3A) as quantified by the lipidomic approach. Detailed analysis of the FA composition of total FA revealed significant reductions in the abundance of C16:0, C18:0, and C18:1 (Figure 3B), all of which are known to be massively scavenged from the host.[4,12] We then sought to determine which lipid species were potentially affected by the loss of *Pf*LPL3 and the reduction in FA content. We therefore analyzed the content of major FA-containing lipids, i.e., (1) neutral lipids making the bulk of lipid bodies/storage lipids, DAG and TAG; (2) PLs and major membrane lipids; and (3) FFAs that are used as building blocks for both neutral lipids and PLs. The abundance of TAGs, DAGs, and PLs was significantly lower in the absence of *Pf*LPL3, whereas the abundance of FFA was significantly increased, together confirming the important role of *Pf*LPL3 for parasite membrane biogenesis (Figure 3C). Importantly, the relative abundance profiles (in mol %) revealed that there was a significant decrease of TAGs and DAGs, whereas FFA and PLs were significantly increasing in the absence of *Pf*LPL3 (Figure 3D). This indicates that the downregulation of *Pf*LPL3 induces an accumulation of FFA and a decrease in the synthesis of TAGs and DAGs in favor of the synthesis of PLs instead. Further, TAG, DAG, and PL composition analyses confirmed that it was the bulk of each lipid class that was impacted by the loss of *Pf*LPL3 rather than specific molecular species (Figure S6), again emphasizing the central role of *Pf*LPL3 for parasite membrane homeostasis. Further analysis of the neutral lipid content shows that both the real and the relative abundance of the TAG/DAG ratio is significantly reduced in the absence of *Pf*LPL3 (Figure 3E), showing that a decrease in TAG following *Pf*LPL3 induces a concomitant decrease in parasite DAG content.

Developing a robust LPL enzymatic assay and identification of potent inhibitors against *Pf*LPL3

To determine the enzymatic activity of *Pf*LPL3, we expressed a recombinant protein corresponding to its LPL/hydrolase domain (41–338 aa). The corresponding recombinant protein was purified, which migrated on SDS-PAGE at the predicted size of ~70 kDa (Figure S7A). The purified recombinant *Pf*LPL3 was used to standardize a fluorescent-based activity assay to quantify its putative LPL activity, using LPC as a standard substrate (Figure S7B). The recombinant *Pf*LPL3 showed concentration-dependent LPL activity in the assay (Figure S7C), confirming the predicted activity of *Pf*LPL3, and more specifically on LPC. The K_M and V_{max} values for *Pf*LPL3 were found to be 49.25 μM and 13,113 nM/min/mg, respectively (Figure S7D). This result confirmed the LPL activity of the enzyme. The recombinant MBP (maltose binding protein) was purified in the same way as was used as a negative control and did not show any enzymatic activity. The *Z* value for the activity assay was found to be ~0.9, showing the robustness of this activity assay, thus also suggesting it could be used for high-throughput screening of compounds (Figures S7E and S7F). Therefore, to identify putative inhibitors of *Pf*LPL3, we screened the MMV antimalarial compounds, "Malaria Box." Interestingly, two compounds, MMV009015 and MMV665796, named as PCB6 and PCB7, respectively, were initially identified with a >75% inhibition of *Pf*LPL3 enzyme activity at 5μM concentration (Figure S7G). We then determined the corresponding IC_{50} values (inhibitory concentration that kills 50% of the parasites) of these compounds to be 1.26 and 0.92 μM, respectively (Figure 4A). Their K_i values were found to be 0.634 and 0.464 μM, respectively, which are less than the respective IC_{50} values, suggesting competitive inhibition by these compounds. The modified K_M values of enzyme in the presence of inhibitor (IC_{50}) were found to be 147.1 and 146.9 μM for PCB6 and PCB7, respectively.

*Pf*LPL3 inhibitors block *P. falciparum* schizont development

The two "Malaria Box" compounds PCB6 and PCB7 are known to show parasiticidal efficacies with the half maximum efficiency concentration, EC_{50} at low micromolar range (Figure 4A). We confirmed the EC_{50} of PCB6 and PCB7 compounds to be 1.26 and 0.9 μM, respectively (Figure 4A). Both inhibitors were assessed for their effect throughout parasite developmental cell cycle during asexual blood stages. It was found that treatment with compounds PCB6 and PCB7 led to normal parasites development from ring to trophozoites/late trophozoite, similar to the solvent control (Figure 4B). However, >50% of these trophozoites were not able to fully develop into mature schizonts, with their morphology appearing deeply affected. The morphological changes of parasites treated by PCB6 and PCB7 both timely coincided and phenocopied the morphological effect observed in *Pf*LPL3 knockdown (Figure 4B). These results strongly indicate the specificity of these compounds for *Pf*LPL3. Both compounds therefore displayed promising antimalarial activity, and their mechanism of action is likely by targeting *Pf*LPL3 and its central function for parasite membrane biogenesis and progeny formation during the schizont stages.

We also assessed any effect of inhibition of *Pf*LPL3 on gametocyte formation using standard gametocyte development assays.[7] However, inhibition of *Pf*LPL3 by PCB6, as well as by PCB7, had no effect on the fraction of gametocytes developed in the assay (Figure S8). These results highlight a specific effect

Figure 3. Lipidomic analyses reveal the role of *Pf*LPL3 to generate FAs and regulate diacylglycerol-triacylglycerol (DAG-TAG) content vs. phospholipid content

Synchronous transgenic parasites at ring stages were grown until late-trophozoite stages (32 h postinfection), and lipid composition was assessed by mass spectrometry-based lipidomic analyses from *Pf*LPL3-iKD and control sets. Data are shown from six independent biological replicates (n = 6).

(A) Total fatty acid (FA) abundance (in nmol lipid/10^7 parasites) reveal a significant decrease of total lipids in *Pf*LPL3-iKD.

(B) Profile of FA species in the 3D7 control and PfLPL3-iKD strains. There was a significant decrease in C160:0, C18:0, and C18:1 in the *Pf*LPL-iKD.

(C) Quantification of the abundance (nmol) in TAGs, DAGs, FFAs, and PLs between *Pf*LPL-iKD and control parasites is revealed.

(D) Relative abundance of TAGs, DAGs, FFAs, and PLs showed significant decreases in TAGs and DAGs, whereas there was a significant increase in FFAs and PLs. Right panels are enlarged sections of the left panel.

(E) Relative abundance of TAG/DAG ratio in *Pf*LPL3-iKD parasites as compared with the control set.

For all assays, the datasets were compared using unpaired Student's t test, and p values are marked: *$p \leq 0.05$, **$p < 0.005$.

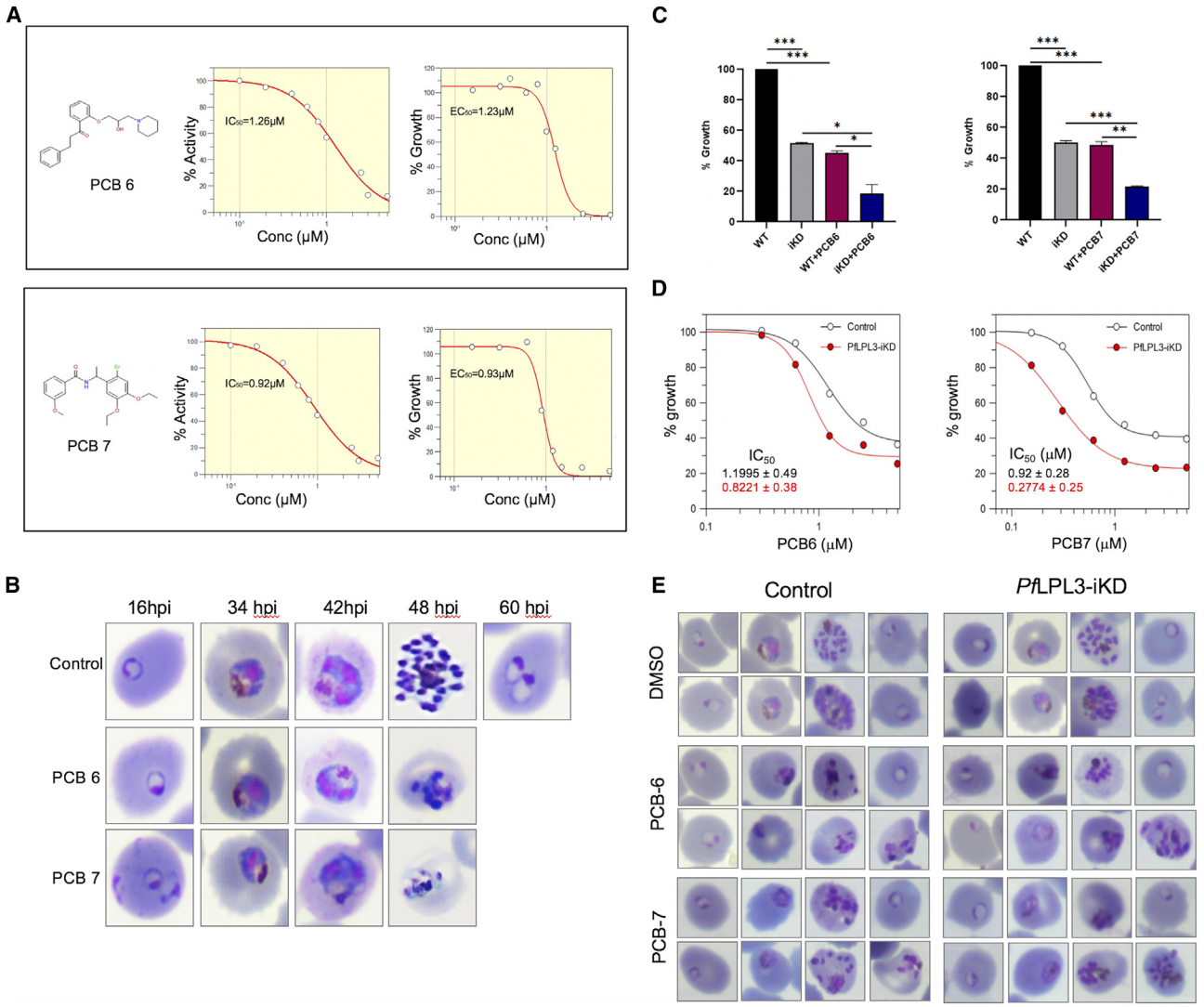

Figure 4. Identification of *Pf*LPL3-specific inhibitors from MMV Malaria Box

A robust *in vitro* activity assay was used to screen the "Malaria Box," and potent inhibitors of *Pf*LPL3 are identified having parasiticidal efficacies.

(A) Concentration-dependent inhibition of enzymatic activity and inhibition of asexual-stage parasite growth by PCB6 (MMV009015) and PCB7 (MMV665796) compounds, respectively. The IC_{50} values (enzyme inhibition) and EC_{50} values (parasite growth inhibition) for both compounds are indicated. All assays were carried out in triplicate.

(B) Effect on the morphology of *P. falciparum* parasites at different time points after treatment with *Pf*LPL3 inhibitors PCB6 and PCB7 at a concentration of EC_{50} values.

(C–E) Effect of *Pf*LPL3 inhibitors, PCB6 and PCB7, on the *Pf*LPL3-iKD parasites to show synergistic effect with *Pf*LPL3-iKD. Synchronized parasite cultures for control and PfLPL3-iKD sets were grown in the presence or absence of *Pf*LPL3 inhibitor (approximate EC_{50} concentration); percentage growth was calculated based on new ring-stage parasites as compared with control. (C) Graph showing % parasite growth in control and *Pf*LPL3-iKD sets alone or with *Pf*LPL3 inhibitor (PCB6 or PCB7 at approximate EC_{50} concentration). Error bars show standard deviation; the datasets were compared using unpaired Student's t test, and p values are marked: *$p \leq 0.05$, **$p \leq 0.005$, ***$p \leq 0.001$, ****$p \leq 0.0005$. (D) Graph showing % parasite growth in *Pf*LPL3-iKD sets alone or in the presence of gradient of concentration of *Pf*LPL3 inhibitor (PCB6 or PCB7) and showing reduced EC_{50} of the respective inhibitor under *Pf*LPL3-iKD conditions. (E) Effect on the morphology of *P. falciparum* parasites at different time points after treatment with *Pf*LPL3 inhibitors PCB6 and PCB7 at a concentration of EC_{50} values for control and *Pf*LPL3-iKD sets.

of these inhibitors on blood stages only. Further, we also evaluated selected hit compounds for their potential to generate drug-resistant parasite populations *in vitro*. A stepwise resistance selection method was implemented.[13,14] No viable parasites were observed after 3 days into the selection step at the >EC_{50} concentration for respective compounds. The parasites obtained from selection in drug (at concentration approximately EC_{50}) were assessed for any change in the EC_{50} for each of the respective compounds, but no significant changes were found in the EC_{50} for PCB6 and PCB7 compounds (Figure S9).

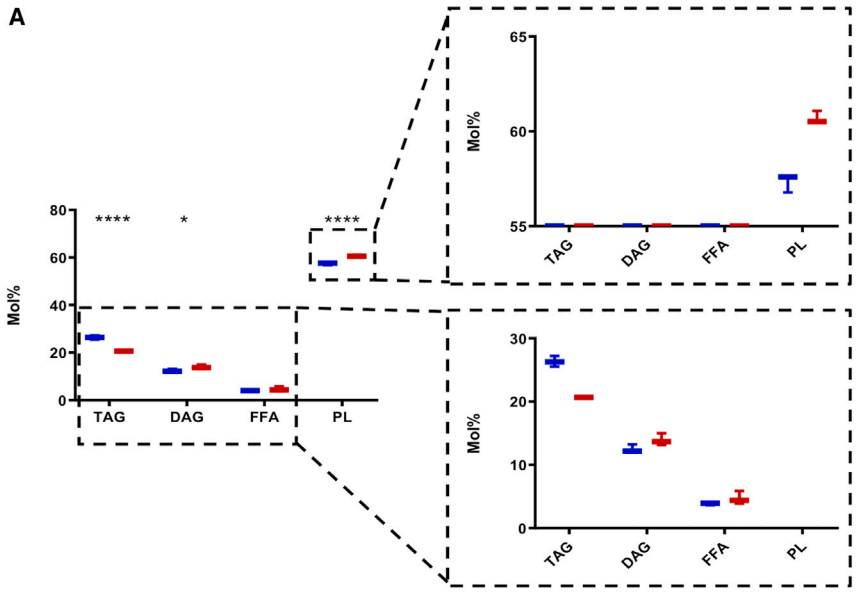

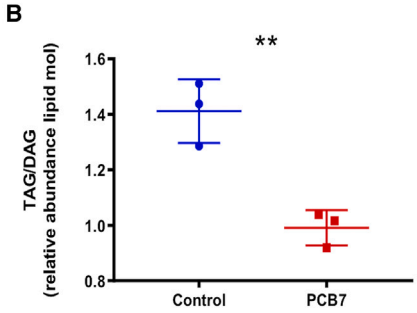

Figure 5. Lipidomic analyses of parasite treated with *Pf*LPL3-specific inhibitors

Synchronous parasites at ring stages were grown until late-trophozoite stages (32 h postinfection) in the presence of inhibitor PCB7 (at concentration approximately IC_{50}), and lipid composition was assessed by mass spectrometry-based lipidomic analyses from inhibitor-treated set as compared with control set. Data are shown from three independent biological replicates (n = 3).

(A) Relative abundance of TAGs, DAGs, FFAs, and PLs showed significant decreases in neutral lipids (TAGs), whereas there was a significant increase in FFAs and PLs. Right panels are enlarged sections of the left panel.

(B) Relative abundance of TAG/DAG ratio in drug-treated parasites as compared with control set.

For all assays, the datasets were compared using unpaired Student's t test, and p values are marked: *$p \leq 0.05$, **$p \leq 0.005$, ***$p \leq 0.001$, ****$p \leq 0.0005$.

*Pf*LPL3 inhibitors show a synergistic effect with *Pf*LPL3-iKD

To further confirm the specificity of identified inhibitors, we assess their additive/synergistic effect with inducible knockdown of *Pf*LPL3 in inhibiting parasite growth. Transgenic parasites in *Pf*LPL3-iKD and control sets were treated with *Pf*LPL3 inhibitors. As stated above, knockdown of *Pf*LPL3 (*Pf*LPL3-iKD set) resulted in ~50% growth reduction. Similarly, treatment with *Pf*LPL3 inhibitors (approximately IC_{50} concentration) showed ~50% growth reduction. In the *Pf*LPL3 inducible knockdown set, the inhibitors showed higher effectiveness, causing ~80% inhibition. These effects are higher than the additive effect of *Pf*LPL3-iKD and respective inhibitors (Figure 4C). Further, we also analyzed the concentration-response curves for both the compounds under control and iKD sets, which showed a gain of sensitivity across multiple concentrations of each of the compounds and change in IC_{50} values (Figure 4D). Morphological analysis of parasite intracellular development using a Giemsa-stained smear showed extensive developmental abnormalities *Pf*LPL3-iKD + inhibitor sets. Specifically, >80% of parasites showed developmental abnormalities in late trophozoites and schizonts, which included having smaller, pyknotic, or sick-looking parasites (Figure 4E). In addition, almost all the schizonts showed a drastic reduction number of merozoites and showed drastic defects in replicative fitness. The overall treatment of *Pf*LPL3-specific inhibitors augmented the morphological effects caused by inducible knockdown of *Pf*LPL3.

*Pf*LPL3 inhibitors disrupt lipid homeostasis through a similar mechanism as in the absence of *Pf*LPL3

To further assess the specificity of identified inhibitors of *Pf*LPL3 on the parasite, we carried out lipidomic analyses of parasite treated with *Pf*LPL3 inhibitor PCB7. The effect of the inhibitor phenocopied the ones induced through the loss of the protein in the knockdown parasite line. Similarly, as for *Pf*LPL3-iKD, the relative abundance profiles (in mol %) showed a significant decrease of neutral lipids, TAGs, whereas FFAs and PLs were significantly increased (Figure 5A). This further indicated that inhibition of *Pf*LPL3 induces an accumulation of FFA and a decrease in the synthesis of neutral lipids in favor of the synthesis of PL instead (Figure 5A). Further, analysis of the neutral lipid content shows that the TAG/DAG ratio is significantly reduced when *Pf*LPL3 is targeted with specific inhibitors also similar to *Pf*LPL3 disruption (Figure 5B). Overall, the lipidomic analysis parasite specificity of the inhibitors on *Pf*LPL3 in the parasite further confirmed the role of *Pf*LPL3 in maintaining lipid homeostasis.

*Pf*LPL3 downregulation or inhibition hampers host-derived lysophospholipids utilization in the parasites

To strengthen the hypothesis that host PLs are being hydrolyzed by *Pf*LPL3, we carried out lipid flux analysis by providing fluorescent-labeled lysophospholipid in the culture medium, as a quantifiable host-scavenged substrate for *Pf*LPL3. The *Pf*LPL3-iKD and control set of parasites were both grown in the presence

of fluorescently labeled lipid lysoPC12:0. To exclude the possibility that parasites were generally less capable for importing lipids, we analyzed parasites specifically during trophozoite stages, when there is no parasite growth phenotype or cellular affection from the loss of *Pf*LPL3 but rather when the peak of *Pf*LPL3 activity is expected. We conducted fluorescence microscopy and flow cytometry to assess and quantify the uptake/utilization of labeled lysophospholipids. As shown in Figure 6A, the control set showed faint labeling of the PV region in the parasites, whereas in the *Pf*LPL3-iKD set, the parasites showed intense labeling of PV regions, indicating the accumulation of unused labeled lipids in the parasite PV. Flow cytometry analysis clearly showed a significant increase in labeling in the parasite population (Figures 6B and 6C). Taken together, these data point at the most likely role of PfPL3 for using lysolipids and providing FA to the parasite at host-parasite interfaces

In parallel experiments, to assess the same effect in MMV drug-treated parasites, we treated *P. falciparum* 3D7 parasite cultures with *Pf*LPL3-specific inhibitors, PCB6 and PCB7, and carried out lipid flux analysis in a similar way. The control and treated sets of parasites were grown in the presence of fluorescently labeled lipid. The control set showed very little or faint labeling of the PV region in the parasites, whereas in the treated set, almost all the parasites showed intense labeling of PV, indicating a similar accumulation of unused labeled lipids (Figure 6D). Flow cytometry analysis clearly showed a significant increase in fluorescence labeling of the parasite population (Figures 6E–6G). Further, to ascertain that the labeled lysoPC12:0 is a substrate for *Pf*LPL3, we assessed the activity of recombinant *Pf*LPL3 on the labeled lysoPC 12:0 using the *in vitro* activity assay; the recombinant *Pf*LPL3 showed LPL activity using this substrate as well (Figure S10).

DISCUSSION

A number of studies highlighted that metabolic pathways linked with lipid synthesis, catabolism, and trafficking are essential for the survival of malaria parasite.[15–18] During the intra-erythrocytic cycle of *P. falciparum,* there is a large increase in the PL, neutral lipid, and lipid-associated FA contents in the infected red blood cells.[4,5,19] Indeed, the parasites require a large amount of lipids to synthesize new membrane-bound organelles, as well as for the assembly of new merozoites after cell division.[20–22] The parasites *de novo* synthesize and scavenge lipids/PLs from the host milieu during the erythrocytic cycle to fulfill this massive requirement of lipids. PLs play a central role in the progression of the life cycle of every parasite and its pathogenesis. Lysophospholipids, especially LPCs, are highly present in the host-cell external environment and are actively scavenged by intra-erythrocytic parasites. Importantly, LPCs serve as major substrates for PL synthesis via the Kennedy pathway through the generation of choline for further PC synthesis and concomitant de-acylation (i.e., loss of their FA chain) putatively catalyzed by the action of unknown LPL.[7,8] The nature of the involved phospholipases and their exact function during parasite development are currently unknown. Interestingly, an unusually high number of LPLs have been identified in the *P. falciparum* genome; however, their putative roles, functions, and localizations remain to be elucidated.

Here, to further understand lipid homeostasis and membrane biosynthesis in the parasite, we explored the role of a putative LPL in *P. falciparum*, *Pf*LPL3, during the asexual life cycle of the parasite. *Pf*LPL3 is a member of the LPL family in the parasite having α/β hydrolases domain and the GXSXG motif, which is the characteristic feature of LPLs. We carried out detailed localization and functional studies to understand the role of *Pf*LPL3 in the parasite. A number of genetic tools have been developed for transient downregulation of target proteins in *Plasmodium* by tagging native genes.[23–25] Here we have tagged the native gene at the C terminus with GFP and a ribozyme system,[10] which was used for both localization and transient knockdown of the target. *Pf*LPL3 was localized at the PV and in the TVN extensions within the host erythrocyte. The PV regions are at the interphase of host-parasite interaction during intracellular growth and are the site of active transport of material from the host to the parasite through PVM. The PVM acts as a molecular sieve for the parasite, whereas TVNs are extensions of PVM, which increases the surface area of the PVM to facilitate more nutrient uptake and protein transport. Based on its putative function, the presence of *Pf*LPL3 in PV is quite intuitive and reveals that the PV/TVN regions are also sites for PL uptake and metabolism. Glycerophosphodiesterases are enzymes that can act downstream of LPL and remove the choline moiety from glycerophospholipids. A recent study[26] shows a tripartite distribution of glycerophosphodiesterase in the cytosol, PV, and food vacuole. The presence of glycerophosphodiesterase, as well as LPL, *Pf*LPL3, in the PV and therefore of the parasite, confirms this area as a major site for the catabolism of exogenously imported PLs into FAs and the respective head group.

Transient downregulation of *Pf*LPL3 caused severe disruption in the development of trophozoites into schizonts stages. The trophozoite stage of the parasite is the metabolically most active stage in which the parasite generates and utilizes the available raw materials for organelle biogenesis, daughter merozoite cell formation, cytokinesis, and karyokinesis; all these processes require an extensive amount of lipids and membrane material. Those parasites in the *Pf*LPL3-iKD set, which were able to develop from trophozoite into schizonts, were heavily compromised on the number of merozoites developed, although these merozoites had properly developed membranes. In *P. berghei*, a phospholipase (PbPL) is also shown to be present in the PV, and its depletion causes a defect in the egress from the host hepatocytes.[27] The *Pf*LPL3-iKD inhibited schizont development and reduced replicative fitness of parasites, which resulted in significant parasite growth inhibition. Indeed, a genome-wide mutagenesis screen using the transposon system suggested *Pf*LPL3 as an essential protein for the parasite, having −3.313 MFS (mutagenesis fitness score) and 0.149 MIS (mutagenesis index score).[28]

Intracellular growth and segregation of *Plasmodium* require lipid synthesis, which is essentially needed for new membrane development. PLs are *de novo* synthesized/assembled by the parasite; however, their precursors (FAs and polar heads) are scavenged from the host milieu. It has been shown that depletion in the serum LPC leads to a decrease in the number of merozoites in the rodent malaria model.[7] Host scavenged LPC is essential for PC synthesis in the parasite. PC is generated by the

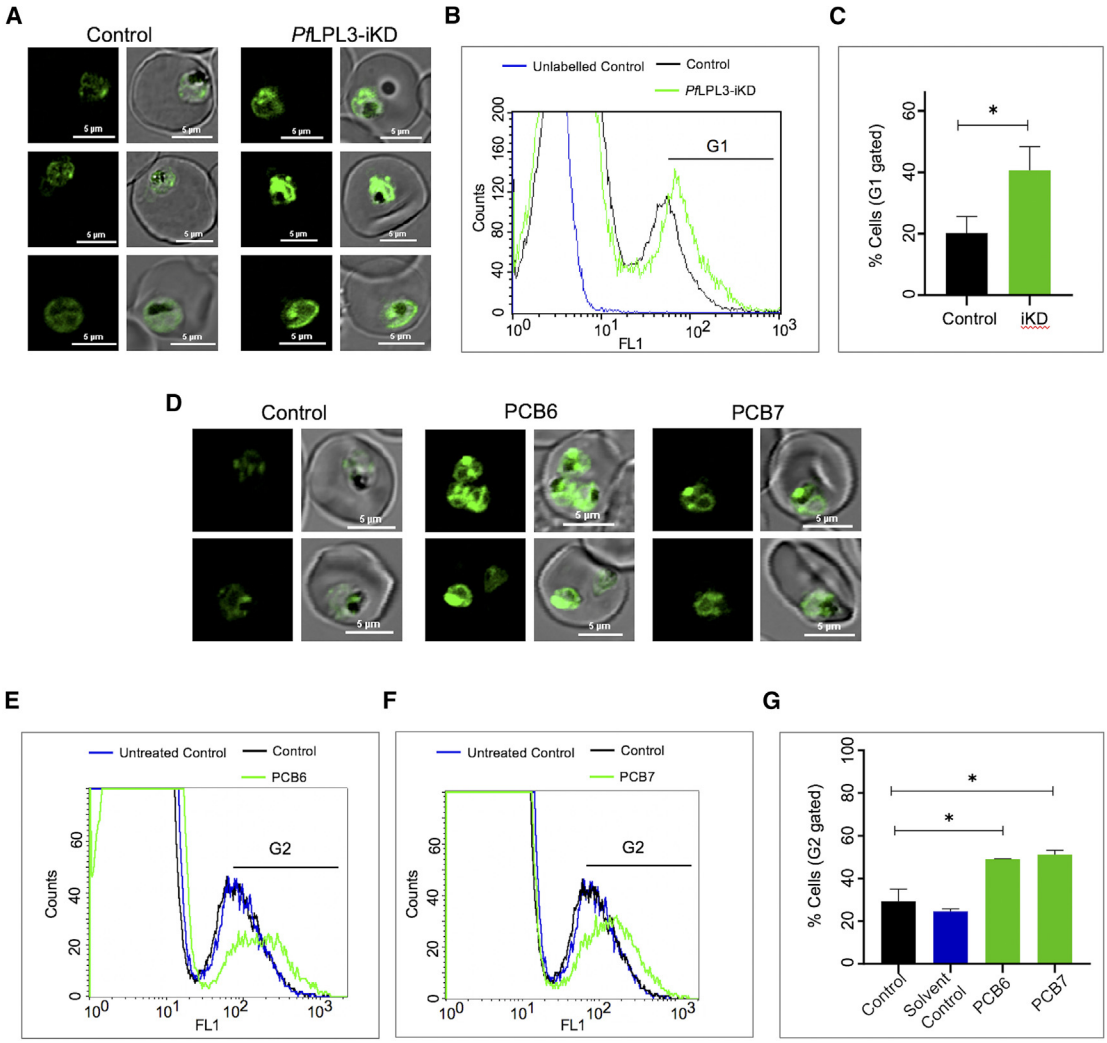

Figure 6. Analysis of fluorescent lysophospholipid flux and trafficking from the host extracellular medium toward the parasite in PfLPL3-iKD

(A) Fluorescence images of control and *Pf*LPL3-iKD parasites grown in the presence of fluorescent-labeled lipid lysoPC12:0. The lipid uptake in the parasite is shown by fluorescence labeling of the parasite, more prominently in the PV, which gets degraded as the lipid is utilized by the parasite; however, in the *Pf*LPL3-iKD set, the fluorescence labeling was seen to be accumulated in the parasite PV as compared with control set. (B) Flow cytometry histogram showing increase in fluorescent population for parasites in *Pf*LPL3-iKD set as compared with control set.

(C) Graph showing % of parasite population in fluorescence gate in the flow cytometry analyses for control and *Pf*LPL3-iKD sets.

(D–G) Lipid flux analysis to show effect of *Pf*LPL3 inhibition by PCB6 and PCB7 inhibitors on utilization of fluorescent-labeled lysophospholipids. (D) Fluorescence images of parasite grown in the presence of fluorescent-labeled lipid lysoPC12:0 and *Pf*LPL3 inhibitor (PCB6 or PCB7) or solvent alone. The labeled lipid showed accumulation in the parasite PV after inhibition of *Pf*LPL3. (E and F) Flow cytometry histograms showing increase in fluorescent population for parasites treated with PCB6 (E) or PCB7 (F) as compared with those treated with solvent alone or untreated set. (G) Graph showing % of parasite population in fluorescence gate in the flow cytometry analyses for control set and parasite treated with PCB6 or PCB7 set. Scale bars represent 5 μm.

Kennedy pathway from CDP-choline,[29,30] whereas in the absence of choline, PC is generated via triple methylation of phosphatidylethanolamine (PE) using ethanolamine and serine as external precursors. Our lipidomic analysis revealed that, beyond being a source for phosphocholine polar heads for PL synthesis, the generation of FA obtained from the utilization of host PC, through the action of *Pf*LPL3, is also crucial for subsequent lipid synthesis for parasite development. Specifically, we found that *Pf*LPL3 functions as a regulator to channel the high rate of FA influx from the host toward neutral lipid DAG and TAG synthesis. Its absence leads to an uncontrolled increase in PL content, most likely blocking the normal development of trophozoite into schizonts and future merozoites. The neutral lipids play important roles in the eukaryotic cell cycle. DAG is known to activate protein kinase C by acting as a second messenger[31]; it also serves as a precursor for the synthesis of TAG and major PLs. TAG is stored in cytosolic lipid droplets that detoxify and sequester FAs, whereas TAG degradation by specific lipase can release these FAs to be utilized for membrane assembly.[32] In asexual-stage parasites, neutral lipids are stored

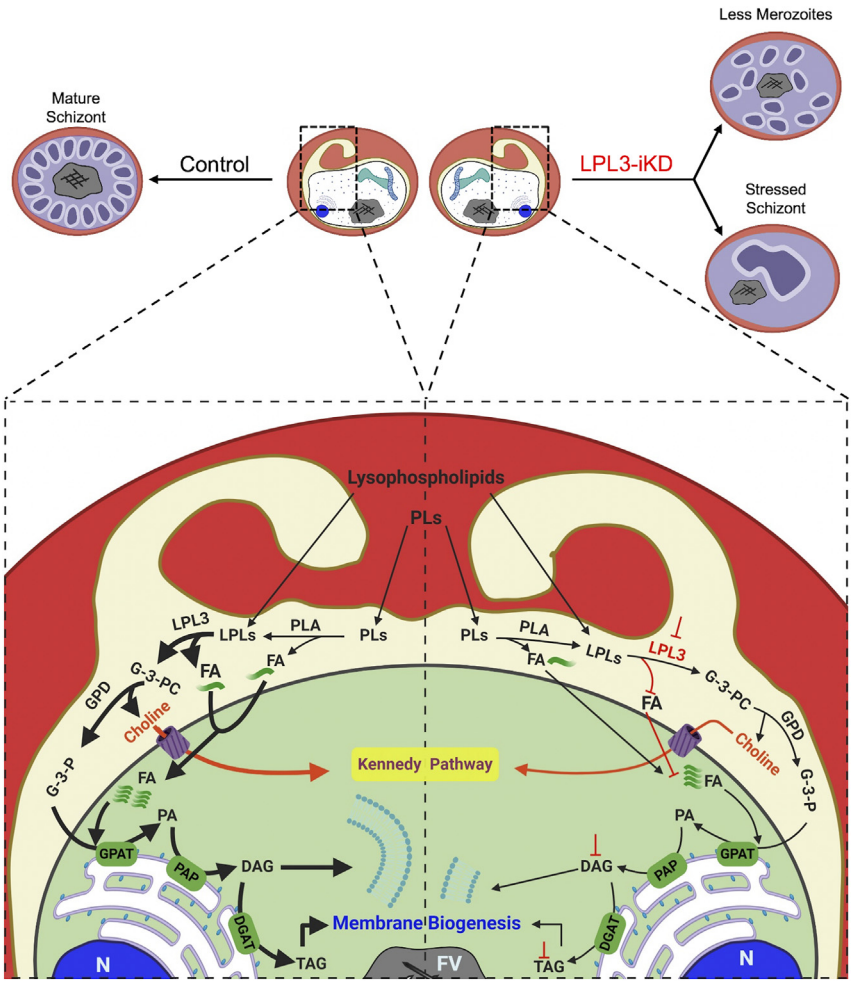

Figure 7. Model of *Pf*LPL3 function in *Plasmodium falciparum* asexual blood-stage cycle

Schematic diagram showing metabolic pathways of lipid metabolism associated with proposed function of *Pf*LPL3. On the left side, *Pf*LPL3 level is maintained in the absence of glucosamine. At the late-trophozoite stage, *Pf*LPL3 localizes in the PV of the parasite, which cleaves the acyl chain from the lysophospholipids (acquired from the host or generated from phospholipid catabolism); this results in generation of glycero-3-phosphate (G-3-P) and FAs, which is ultimately required for DAG and TAG synthesis. In the presence of PfLPL3, neutral lipid and membrane biogenesis are normal, which results in normal schizogony. On the right side, consequences of *Pf*LPL3 knockdown are shown. The decreased level of *Pf*LPL3 in the presence of glucosamine leads to dysregulation of FA content, which disrupts phospholipid synthesis and development of new membranes. Therefore, *Pf*LPL3 knockdown disrupts schizogony and causes reduction in number of merozoites in schizonts. DGAT, diglyceride acyltransferase; FV, food vacuole; G-3-PC, glycero-3-phosphocholine; GPAT, glycerol-3-phosphate acyltransferase; LPL, lysophospholipid; LPL3, lysophospholipase 3; N, nucleus; PA, phosphatidic acid; PAP, phosphatidate phosphatase; PL, phospholipid; PLA, phospholipase A.

in a lipid body associated with the food vacuole.[33,34] During parasite growth, hydrolysis of TAG can rapidly produce FAs to utilize in membrane synthesis.[35] A general lipase inhibitor, Orlistat, was suggested to block the utilization of stored TAGs, which inhibited parasite growth and caused developmental arrest in the late stages.[5] In a similar way, reduction in TAG levels in *Pf*LPL3-iKD conditions caused arrest of the parasite in late stages; in addition, some of the parasites showed a reduced number of merozoites, which points to hindrance in membrane biogenesis. Taken together, this shows a similar strategy between *T. gondii* tachyzoites and *P. falciparum* asexual blood stages to (1) massively acquire host FAs by catabolism of host lipids; (2) channel this FA flux toward lipid storage, TAGs; and (3) control mobilization of these FAs for division purposes.[9] The specific function of *Pf*LPL3 was confirmed by using *in vitro* and in-cell activity assays. The recombinant *Pf*LPL3 was able to specifically hydrolyze lysophospholipids such as LPC. Further, disruption of *Pf*LPL3 caused a specific accumulation of fluorescent lysophospholipid, an expected substrate of the enzyme, in the PV. We confirmed that such fluorescent-labeled lysophospholipid is also a substrate that is specifically recognized and used by *Pf*LPL3, along with LPC. These data clearly show the role of *Pf*LPL3 in the degradation of host scavenged and derived PLs to generate FAs stored as TAGs, then used for growth and division of the parasite during schizogony, as summarized in Figure 7. Overall, our data reveal that during blood stages, *P. falciparum* controls lipid synthesis and consequent formation of daughter cells by (1) favoring generation and storage of FA building blocks through the synthesis of DAG and TAG; and (2) timely allowing the generation of structural PLs for merozoite formation through the utilization of FAs from DAGs and TAGs, rather than constantly accumulating FFAs and/or synthesizing PLs from them, both of which are lipotoxic for the parasite.

One of the important motives for understanding the biology of the parasite is to identify functionally important metabolic pathways as drug targets and subsequently design their specific inhibitors to develop as new antimalarials. Our study involving detailed localization, gene knockdown, and lipidomic analyses clearly shows that *Pf*LPL3 plays a critical role in the growth and segregation of the parasite during the asexual cycle. We also showed that *Pf*LPL3 harbor enzymatic activity for LPL. Furthermore, a robust *in vitro* activity assay was established to screen the compound libraries. MMV established an open, collaborative initiative in search of novel drugs for neglected tropical diseases. Based on an extensive screening strategy, they identified a set of drug-like compounds having antimalarial activity, and they labeled this set as "Malaria Box."[36] These compounds are leads to further develop into antimalarial drugs.

However, there is a need to identify potential targets for these compounds in the parasite, which may help medicinal chemistry approaches to design diversity library and identify potent antimalarials. Screening of the "Malaria Box" by using the *Pf*LPL3 activity assay identified two hit compounds, labeled as PCB6 and PCB7; both compounds have parasiticidal efficacy and block the schizont development in *P. falciparum*, which phenocopies the gene knockdown phenotype, and thus consistently confirms the role of *Pf*LPL3. Further, both compounds showed very close efficacies in inhibiting enzyme activity and parasite growth, IC_{50} and $EC_{50,}$ respectively, in the low micromolar range. These results suggest that both compounds specifically target the *Pf*LPL3 in the asexual-stage parasite. Interestingly, inhibition of *Pf*LPL3 by PCB6, as well as by PCB7, had no effect on gametocytes developed, which highlights a specific role of *Pf*LPL3 during blood stages; indeed, high-throughput screening by Lucantoni et al.[37] showed that the two selected compounds had no significant effect on gametocyte development. The specificity of the target by the selected compound was further confirmed by lipidomic analysis of parasites treated with these compounds. Lipidomic analyses revealed exact similar effects of the inhibitors over parasite lipid homeostasis as parasites lacking *Pf*LPL3 in the knockdown parasite line. In addition, these drugs showed synergistic effects on parasite growth along with the genetic ablation of *Pf*LPL3 ablation, suggesting increased sensitivity for the inhibitors. Indeed, transient knockdown of a target is shown to increase sensitivity to inhibitors specific to that pathway.[38] Our results thus point toward the specificity of the *Pf*LPL3 inhibitors in the parasite. Further, lipid flux analysis showed that treatment with these inhibitors blocks the hydrolysis of complex lipid take-up from the host milieu, as in the case of gene knockdown parasites, confirming the target specificity of these inhibitors. Overall, we believe that the compounds have *Pf*LPL3 as a specific/major target in the parasite based on various datasets: (1) very close values for their IC_{50} on enzyme activity and EC_{50} on parasite growth for the selected compounds; (2) similar morphological effects in gene knockdown and inhibitor treatment; and (3) gain of sensitivity that is apparent across multiple concentrations of the test compounds and change in IC_{50} values in gene knockdown parasites. These specific inhibitors of *Pf*LPL3 can be further developed through a medicinal chemistry campaign into potent antimalarials, in addition to being specific molecular tools to study lipid synthesis and membrane biogenesis during schizogony and merozoite formation.

Limitations of the study

In order to clearly identify PfLPL3 as the target of the MMV compounds, the authors used (1) the accumulation of lysoPC in the parasites as a proxy for *Pf*LPL3 activity; (2) similar accumulation of LPCs in an *in vitro* assay on the recombinant PfLPL3; and (3) the use of fluorescent LPL, which accumulates at the periphery of the parasites in the absence of LPL3 and further controls that fluorescent LPC is also a substrate of LPL3 *in vitro*. Although all of those orthogonal methods specifically point to the fact that PfLPL3 is the substrate for the MMV compounds, one cannot rule out that slow-growing parasites as affected by any drug may have their PL import capacities affected. Such phenotype was never observed before in any reported mutant, and other drug controls did not lead to such similar results as well. The authors tried to generate resistance to the MMV compounds, but this did not work. Further studies could include more resistance assays as to rule out any unspecific activities of the PCB6/7 compounds.

STAR★METHODS

Detailed methods are provided in the online version of this paper and include the following:

- KEY RESOURCES TABLE
- RESOURCE AVAILABILITY
  - Lead contact
  - Materials availability
  - Data and code availability
- EXPERIMENTAL MODEL AND SUBJECT DETAILS
  - Parasite culture, plasmid construct and parasite transfection
- METHOD DETAILS
  - Conditional knock-down and *in-vitro* growth assays analysis
  - Parasite fractionation and western blot analysis
  - Immunofluorescence assay (IFA) and fluorescent microscopy
  - Lipidomic analyses
  - Phospholipid uptake and flux analysis
  - Cloning, expression and purification of recombinant protein
  - Lysophospholipase (LPL) activity assay and enzyme kinetics
  - Standardization of a robust lysophospholipase (LPL) activity assay and screening of compound library
- QUANTIFICATION AND STATISTICAL ANALYSIS

SUPPLEMENTAL INFORMATION

Supplemental information can be found online at https://doi.org/10.1016/j.celrep.2023.112251.

ACKNOWLEDGMENTS

We are grateful to Philip J. Shaw for providing vector pGFP_*glm*S and useful suggestions. We thank Rotary blood bank, New Delhi for providing the RBCs. P.K.S. was supported by a research fellowship from University Grants Commission, Government of India. M.N. was supported by a research fellowship from Department of Biotechnology, Government of India. V.T. was supported by a BioCARe Women Scientist fellowship from Department of Biotechnology, Government of India. M.M.I. was supported by an international pre-doctoral research fellowship from ICGEB. The research work in A.M.'s laboratory was supported by a Centre of Excellence grant (BT/COE/34/SP15138/2015) and Flagship Project grant (BT/IC-06/003/91) from Department of Biotechnology, Government of India. C.Y.B. and Y.Y.-B. were supported by Agence Nationale de la Recherche, France (Project ApicoLipiAdapt grant ANR-21-CE44-0010), The Fondation pour la Recherche Médicale (FRM EQU202103012700), Laboratoire d'Excellence Parafrap, France (grant ANR-11-LABX-0024), LIA-IRP CNRS Program (Apicolipid project), the Université Grenoble Alpes (IDEX ISP Apicolipid), and Région Auvergne-Rhône-Alpes for the lipidomics analyses platform (Grant IRICE Project GEMELI). The current manuscript, the joint international project, and collaboration between the

laboratories of A.M. and C.Y.B. were supported by Indo-French Collaborative Research Program Grant CEFIPRA (Project 6003-1) to A.M. and C.Y.B. by the CEFIPRA (French MESRI and Indian DBT). The funders had no role in study design, data collection and interpretation, or the decision to submit the work for publication. We thank Medicines for Malaria Venture (MMV, Switzerland) for providing the "Malaria Box" compound library, as well as selected compounds.

AUTHOR CONTRIBUTIONS

A.M. and C.Y.B. conceived and designed the study; P.K.S., Y.Y.-B., M.N., V.T., C.S., M.M.I., M.M.B., and M.A. carried out the experiments; A.M., Y.Y.-B., and C.Y.B. analyzed the data; P.K.S., A.M., and C.Y.B. wrote the paper with contributions from all authors.

DECLARATION OF INTERESTS

The authors declare no competing interests.

Received: March 9, 2022
Revised: November 4, 2022
Accepted: February 24, 2023
Published: April 3, 2023

REFERENCES

1. World Health Organisation (2021). World malaria report 2021. https://apps.who.int/iris/handle/10665/350147.
2. Déchamps, S., Wengelnik, K., Berry-Sterkers, L., Cerdan, R., Vial, H.J., and Gannoun-Zaki, L. (2010). The Kennedy phospholipid biosynthesis pathways are refractory to genetic disruption in Plasmodium berghei and therefore appear essential in blood stages. Mol. Biochem. Parasitol. *173*, 69–80.
3. Amiar, S., Katris, N.J., Berry, L., Dass, S., Duley, S., Arnold, C.S., Shears, M.J., Brunet, C., Touquet, B., McFadden, G.I., et al. (2020). Division and adaptation to host environment of apicomplexan parasites depend on apicoplast lipid metabolic plasticity and host organelle remodeling. Cell Rep. *30*, 3778–3792.e9.
4. Botté, C.Y., Yamaryo-Botté, Y., Rupasinghe, T.W.T., Mullin, K.A., MacRae, J.I., Spurck, T.P., Kalanon, M., Shears, M.J., Coppel, R.L., Crellin, P.K., et al. (2013). Atypical lipid composition in the purified relict plastid (apicoplast) of malaria parasites. Proc. Natl. Acad. Sci. USA *110*, 7506–7511.
5. Gulati, S., Ekland, E.H., Ruggles, K.V., Chan, R.B., Jayabalasingham, B., Zhou, B., Mantel, P.Y., Lee, M.C.S., Spottiswoode, N., Coburn-Flynn, O., et al. (2015). Profiling the essential nature of lipid metabolism in asexual blood and gametocyte stages of Plasmodium falciparum. Cell Host Microbe *18*, 371–381.
6. Itoe, M.A., Sampaio, J.L., Cabal, G.G., Real, E., Zuzarte-Luis, V., March, S., Bhatia, S.N., Frischknecht, F., Thiele, C., Shevchenko, A., and Mota, M.M. (2014). Host cell phosphatidylcholine is a key mediator of malaria parasite survival during liver stage infection. Cell Host Microbe *16*, 778–786.
7. Brancucci, N.M.B., Gerdt, J.P., Wang, C., De Niz, M., Philip, N., Adapa, S.R., Zhang, M., Hitz, E., Niederwieser, I., Boltryk, S.D., et al. (2017). Lysophosphatidylcholine regulates sexual stage differentiation in the human malaria parasite Plasmodium falciparum. Cell *171*, 1532–1544.e15.
8. Wein, S., Ghezal, S., Buré, C., Maynadier, M., Périgaud, C., Vial, H.J., Lefebvre-Tournier, I., Wengelnik, K., and Cerdan, R. (2018). Contribution of the precursors and interplay of the pathways in the phospholipid metabolism of the malaria parasite. J. Lipid Res. *59*, 1461–1471.
9. Dass, S., Shunmugam, S., Berry, L., Arnold, C.S., Katris, N.J., Duley, S., Pierrel, F., Cesbron-Delauw, M.F., Yamaryo-Botté, Y., and Botté, C.Y. (2021). Toxoplasma LIPIN is essential in channeling host lipid fluxes through membrane biogenesis and lipid storage. Nat. Commun. *12*, 2813.
10. Prommana, P., Uthaipibull, C., Wongsombat, C., Kamchonwongpaisan, S., Yuthavong, Y., Knuepfer, E., Holder, A.A., and Shaw, P.J. (2013). Inducible knockdown of Plasmodium gene expression using the glmS ribozyme. PLoS One *8*, e73783.
11. Stallmach, R., Kavishwar, M., Withers-Martinez, C., Hackett, F., Collins, C.R., Howell, S.A., Yeoh, S., Knuepfer, E., Atid, A.J., Holder, A.A., and Blackman, M.J. (2015). Plasmodium falciparum SERA5 plays a non-enzymatic role in the malarial asexual blood-stage lifecycle. Mol. Microbiol. *96*, 368–387.
12. Mitamura, T., Hanada, K., Ko-Mitamura, E.P., Nishijima, M., and Horii, T. (2000). Serum factors governing intraerythrocytic development and cell cycle progression of Plasmodium falciparum. Parasitol. Int. *49*, 219–229.
13. Crandall, I.E., Wasilewski, E., Bello, A.M., Mohmmed, A., Malhotra, P., Pai, E.F., Kain, K.C., and Kotra, L.P. (2013). Antimalarial activities of 6-iodouridine and its prodrugs and potential for combination therapy. J. Med. Chem. *56*, 2348–2358.
14. Goodman, C.D., Uddin, T., Spillman, N.J., and McFadden, G.I. (2020). A single point mutation in the Plasmodium falciparum FtsH1 metalloprotease confers actinonin resistance. Elife *9*, e58629.
15. Ben Mamoun, C., Prigge, S.T., and Vial, H. (2010). Targeting the lipid metabolic pathways for the treatment of malaria. Drug Dev. Res. *71*, 44–55.
16. Choubey, V., Maity, P., Guha, M., Kumar, S., Srivastava, K., Puri, S.K., and Bandyopadhyay, U. (2007). Inhibition of Plasmodium falciparum choline kinase by hexadecyltrimethylammonium bromide: a possible antimalarial mechanism. Antimicrob. Agents Chemother. *51*, 696–706.
17. Hanada, K., Palacpac, N.M.Q., Magistrado, P.A., Kurokawa, K., Rai, G., Sakata, D., Hara, T., Horii, T., Nishijima, M., and Mitamura, T. (2002). Plasmodium falciparum phospholipase C hydrolyzing sphingomyelin and lysocholinephospholipids is a possible target for malaria chemotherapy. J. Exp. Med. *195*, 23–34.
18. Mitamura, T., and Palacpac, N.M.Q. (2003). Lipid metabolism in Plasmodium falciparum-infected erythrocytes: possible new targets for malaria chemotherapy. Microbes Infect. *5*, 545–552.
19. Nawabi, P., Lykidis, A., Ji, D., and Haldar, K. (2003). Neutral-lipid analysis reveals elevation of acylglycerols and lack of cholesterol esters in Plasmodium falciparum-infected erythrocytes. Eukaryot. Cell *2*, 1128–1131.
20. Pessi, G., Kociubinski, G., and Mamoun, C.B. (2004). A pathway for phosphatidylcholine biosynthesis in Plasmodium falciparum involving phosphoethanolamine methylation. Proc. Natl. Acad. Sci. USA *101*, 6206–6211.
21. Ramakrishnan, S., Serricchio, M., Striepen, B., and Bütikofer, P. (2013). Lipid synthesis in protozoan parasites: a comparison between kinetoplastids and apicomplexans. Prog. Lipid Res. *52*, 488–512.
22. Witola, W.H., El Bissati, K., Pessi, G., Xie, C., Roepe, P.D., and Mamoun, C.B. (2008). Disruption of the Plasmodium falciparum PfPMT gene results in a complete loss of phosphatidylcholine biosynthesis via the serine-decarboxylase-phosphoethanolamine-methyltransferase pathway and severe growth and survival defects. J. Biol. Chem. *283*, 27636–27643.
23. Armstrong, C.M., and Goldberg, D.E. (2007). An FKBP destabilization domain modulates protein levels in Plasmodium falciparum. Nat. Methods *4*, 1007–1009.
24. de Koning-Ward, T.F., Gilson, P.R., and Crabb, B.S. (2015). Advances in molecular genetic systems in malaria. Nat. Rev. Microbiol. *13*, 373–387.
25. Meissner, M., Krejany, E., Gilson, P.R., de Koning-Ward, T.F., Soldati, D., and Crabb, B.S. (2005). Tetracycline analogue-regulated transgene expression in Plasmodium falciparum blood stages using Toxoplasma gondii transactivators. Proc. Natl. Acad. Sci. USA *102*, 2980–2985.
26. Denloye, T., Dalal, S., and Klemba, M. (2012). Characterization of a glycerophosphodiesterase with an unusual tripartite distribution and an important role in the asexual blood stages of Plasmodium falciparum. Mol. Biochem. Parasitol. *186*, 29–37.
27. Burda, P.C., Roelli, M.A., Schaffner, M., Khan, S.M., Janse, C.J., and Heussler, V.T. (2015). A Plasmodium phospholipase is involved in

disruption of the liver stage parasitophorous vacuole membrane. PLoS Pathog. *11*, e1004760.

28. Zhang, M., Wang, C., Otto, T.D., Oberstaller, J., Liao, X., Adapa, S.R., Udenze, K., Bronner, I.F., Casandra, D., Mayho, M., et al. (2018). Uncovering the essential genes of the human malaria parasite Plasmodium falciparum by saturation mutagenesis. Science *360*, eaap7847.
29. Flammersfeld, A., Lang, C., Flieger, A., and Pradel, G. (2018). Phospholipases during membrane dynamics in malaria parasites. Int. J. Med. Microbiol. *308*, 129–141.
30. Tischer, M., Pradel, G., Ohlsen, K., and Holzgrabe, U. (2012). Quaternary ammonium salts and their antimicrobial potential: targets or nonspecific interactions? ChemMedChem *7*, 22–31.
31. Goñi, F.M., and Alonso, A. (1999). Structure and functional properties of diacylglycerols in membranes. Prog. Lipid Res. *38*, 1–48.
32. Athenstaedt, K., and Daum, G. (2006). The life cycle of neutral lipids: synthesis, storage and degradation. Cell. Mol. Life Sci. *63*, 1355–1369.
33. Asad, M., Yamaryo-Botté, Y., Hossain, M.E., Thakur, V., Jain, S., Datta, G., Botté, C.Y., and Mohmmed, A. (2021). An essential vesicular-trafficking phospholipase mediates neutral lipid synthesis and contributes to hemozoin formation in Plasmodium falciparum. BMC Biol. *19*, 159.
34. Jackson, K.E., Klonis, N., Ferguson, D.J.P., Adisa, A., Dogovski, C., and Tilley, L. (2004). Food vacuole-associated lipid bodies and heterogeneous lipid environments in the malaria parasite, Plasmodium falciparum. Mol. Microbiol. *54*, 109–122.
35. Palacpac, N.M.Q., Hiramine, Y., Mi-ichi, F., Torii, M., Kita, K., Hiramatsu, R., Horii, T., and Mitamura, T. (2004). Developmental-stage-specific triacylglycerol biosynthesis, degradation and trafficking as lipid bodies in Plasmodium falciparum-infected erythrocytes. J. Cell Sci. *117* (*Pt 8*), 1469–1480.
36. Spangenberg, T., Burrows, J.N., Kowalczyk, P., McDonald, S., Wells, T.N.C., and Willis, P. (2013). The open access malaria box: a drug discovery catalyst for neglected diseases. PLoS One *8*, e62906.
37. Lucantoni, L., Silvestrini, F., Signore, M., Siciliano, G., Eldering, M., Dechering, K.J., Avery, V.M., and Alano, P. (2015). A simple and predictive phenotypic High Content Imaging assay for Plasmodium falciparum mature gametocytes to identify malaria transmission blocking compounds. Sci. Rep. *5*, 16414.
38. Lu, K.Y., Pasaje, C.F.A., Srivastava, T., Loiselle, D.R., Niles, J.C., and Derbyshire, E. (2020). Phosphatidylinositol 3-phosphate and Hsp70 protect Plasmodium falciparum from heat-induced cell death. Elife *9*, e56773.
39. Paul, G., Deshmukh, A., Kaur, I., Rathore, S., Dabral, S., Panda, A., Singh, S.K., Mohmmed, A., Theisen, M., and Malhotra, P. (2017). A novel Pfs38 protein complex on the surface of Plasmodium falciparum blood-stage merozoites. Malar. J. *16*, 79.
40. Dubois, D., Fernandes, S., Amiar, S., Dass, S., Katris, N.J., Botté, C.Y., and Yamaryo-Botté, Y. (2018). Toxoplasma gondii acetyl-CoA synthetase is involved in fatty acid elongation (of long fatty acid chains) during tachyzoite life stages. J. Lipid Res. *59*, 994–1004.
41. Zhang, J.H., Chung, T.D., and Oldenburg, K.R. (1999). A simple statistical parameter for use in evaluation and validation of high throughput screening assays. J. Biomol. Screen *4*, 67–73.

STAR★METHODS

KEY RESOURCES TABLE

REAGENT or RESOURCE	SOURCE	IDENTIFIER
Antibodies		
Anti-GFP antibody	Roche	Cat# 11814460001
Anti-rabbit HRP conjugated secondary antibody	Sigma	Cat# 12-348
Monoclonal anti-spectrin	Sigma	Cat# S3396
Mice polyclonal anti-SERA5	Paul et al.[39]	NA
Rabbit anti-BiP	Asad et al.[33]	NA
Anti-MSP1 antibody	Paul et al.[39]	NA
Chemicals, peptides, and recombinant proteins		
Glucosamine	Sigma	Cat# G4875
RPMI media	Invitrogen	Cat# 31800022
Albumax	Invitrogen	Cat# 11021029
Gentamicin	Invitrogen	Cat# 15710064
Blasticidin S	Calbiochem	Cat# 203350
DAPI	Sigma	Cat# D9542
LysoPC 12:0 with NBD label	Avanti Polar Lipids, Inc	Cat# 810128
16:0 Lysophosphatidylcholine (LPC)	Avanti Polar Lipids, Inc	Cat# 855675
Glycerophosphodiesterase	Sigma	Cat# G1642
Choline oxidase	Sigma	Cat# 26978
Horseradish peroxidase	Sigma	Cat# P8125
Amplex Red	Invitrogen	Cat# A12222
Critical commercial assays		
ECL Western Blotting Substrate	Pierce™, Thermo Scientific	Cat# 32106
Experimental models: Cell lines		
E. coli BL21(DE3) codon$^+$ cells	Novagen	Cat# 69450
Experimental models: Organisms/strains		
Plasmodium falciparum strain 3D7	MR4	Cat# MRA-102
P. falciparum 3D7 PLP3 knock-down, *Pf*LPL3_GFP_glmS	This study	NA
Oligonucleotides		
For primers and oligonucleotides, see Table S1	See Table S1	NA
Recombinant DNA		
*Pf*LPL3_GFP_*glm*S (Plasmid construct)	This study	NA
Software and algorithms		
GraphPad Prism ver. 5.0	https://www.graphpad.com/scientific-software/prism/	NA
BD Cell Quest Pro	Beckton Dickinson	NA
IMARIS ver. 7.0	Bitplane Scientific	NA

RESOURCE AVAILABILITY

Lead contact

Further information and requests for resources and reagents should be directed to and will be fulfilled by the lead contacts, Dr Cyrille Botté (cyrille.botte@univ-grenoble-alpes.fr), and Dr Asif Mohmmed (amohd@icgeb.res.in).

Materials availability

All unique material generated for this work can be shared upon request to the corresponding authors.

Data and code availability

All data generated in this paper can be shared upon request to the corresponding authors. This paper does not report original code. Any additional information required to reanalyze the data reported in this paper can be made available upon request.

EXPERIMENTAL MODEL AND SUBJECT DETAILS

All experiments were carried out on Plasmodium falciparum 3D7 stain.

Parasite culture, plasmid construct and parasite transfection

Plasmodium falciparum strain 3D7 was cultured in RPMI media (Invitrogen) supplemented with 0.5% (w/v) Albumax^{TM} (Invitrogen) 4% haematocrit. Culture was kept static in a gas mixture of 5% carbon dioxide, 5% oxygen and 90% nitrogen at 37°C. To generate *Pf*LPL3_GFP_*glm*S construct, a C-terminal fragment (702 base pair) of *pfLPL3* gene was amplified using specific primers 1222A and 1223A (Table S1) and cloned in to GFP_*glm*S vector.[10] The C-terminal fragment was cloned in frame to the N-terminus of GFP in the *Spe*I and *Kpn*I restriction enzymes sites. Parasite cultures were synchronized by repeated sorbitol treatment and 100 μg of purified plasmid DNA (Plasmid Midi Kit, Qiagen, Valencia, CA) was transfected in *P. falciparum* by electroporation (310 V, 950 μF). Transfected parasites were selected over 2.5 μg/mL blasticidin (Calbiochem) and subsequently subjected to on and off cycling of blasticidin drug to promote integration of the plasmid in the main genome. Integration was confirmed by PCR using 1270A and 1234A and by western blotting also by using anti-GFP antibody.

METHOD DETAILS

Conditional knock-down and *in-vitro* growth assays analysis

To assess the effect of knock-down of *Pf*LPL3 on parasite, *Pf*LPL3_ GFP_*glm*S transgenic parasites were tightly synchronized with 5% sorbitol and treated with 2.5mM of glucosamine (Sigma-Aldrich) in 24 well plates containing 4% hematocrit and 1% parasitemia at ring stages (18–20pi). For microscopic analysis and morphology of the parasites, Giemsa stained smears were prepared at every 8 h interval, from both glucosamine treated and control sets. Parasite growth was assessed at 48 and 96 h after the addition of glucosamine by flow cytometry using BD FACS Calibur (Beckton Dickinson); briefly, cells were incubated with EtBr for 30 min at 37°C in dark and after two washing with PBS, 100000 events were acquired using BD FACS Calibur system (Beckton Dickinson). To determine merozoite frequency in schizont stage parasites, number of merozoites in schizonts of parasite cultures in iKD set and control set were counted (n = 50), and the data was presented as number of parasites having different numbers of merozoites/schizont. To assess the effect of glucosamine on the down regulation of *Pf*LPL3 at protein level, *Pf*LPL3_GFP_*glm*S ring stage parasites (18–20hpi) were grown in presence of glucosamine (2.5mM), harvested at late-trophozoite/schizont stages (36–40hpi), and subjected to the western blotting.

Parasite fractionation and western blot analysis

Parasites were harvested at trophozoite stage using 0.15% saponin for RBC lysis, the supernatant was collected, and parasites pellet was lysed by freeze-thaw cycle. Laemmli buffer was added to both the fractions and proteins were separated in 12% SDS-PAGE; the proteins were transferred to PVDF membrane (Millipore) and incubated with blocking buffer (4% skim milk in 1× PBS) followed by incubation with the primary antibody: (monoclonal anti-GFP mice 1:5000 (Roche), rabbit anti-GFP 1:10000, rabbit anti-BiP 1:15000 or monoclonal anti-spectrin 1:1000). Blots were washed 5 times with 1 PBS, probed with HRP conjugated secondary antibody (1:100000) and visualized using ECL detection kit (Thermo-scientific).

Immunofluorescence assay (IFA) and fluorescent microscopy

The parasites were fixed in 4% paraformaldehyde. After permeabilization with 0.1% Triton X-100, 10% bovine serum was used for blocking; cells were incubated with rabbit polyclonal anti-GFP (1:500) or mice polyclonal anti-SERA5 (1:500), or mice anti-MSP1 (1:500) for 2 h and subsequently with Alexa Flour-488 and- 594 labeled secondary antibody. Labeled parasites were washed three times with 1× PBS. Parasite nuclei were stained with DAPI at a final concentration of 5 μg/mL. The membrane structures in parasitized erythrocytes were labeled with BODIPY TR-ceramide (Invitrogen) with a final concentration of 1μM. Images were captured by Nikon A1 confocal laser scanning microscope and analyzed by Nikon-nis element software (version 4.1). The 3D images were constructed by using series of z stack images and IMARIS 7.0 (Bitplane Scientific) software.

Lipidomic analyses

Total lipids were extracted from treated (*Pf*LPL3-iKD) and control parasites. First parasites (4×10^8 cell equivalents) were harvested by using 0.15% saponin treatment. These parasites were metabolically quenched by rapid chilling in a dry ice-ethanol slurry bath and then centrifuged down at 4°C. The parasite pellet obtained was washed with ice-cold PBS thrice, before transferring the final pellet to

a microcentrifuge tube. The total lipid samples were spiked with 20 nmol C21:0 phosphatidylcholine, and extracted by chloroform: methanol, 1:2(v/v) and chloroform: methanol, 2:1 (v/v). The pooled organic phase was subjected to biphasic separation by adding 0.1% KCl and was then dried under N_2 gas flux prior to being dissolved in 1-butanol.

Total lipid analysis

Total lipid was then added with 1 nmol pentadecanoic acid (C15:0) as internal standard and derivatized to give fatty acid methyl ester (FAME) using on-line using MethPrep II (Alltech) and the resulting FAMEs were extracted using hexane. Resultant FAMEs were then analyzed by GC-MS as previously described.[40] All FAMEs were identified by comparison of retention time and mass spectra from GC-MS with authentic chemical standards. The concentration of FAMEs was quantified after initial normalization to different internal standards and finally to parasite number.

Phospholipid and neutral lipid analysis

For phospholipid analysis, total lipid extracted (as mentioned above) was separated with 1 nmol PA(C17:0/C17:0) (Avanti Polar lipids) by one-dimensional silica gel high-performance thin-layer chromatography (HPTLC, Merck). Total PL, DAG, TAG, Free fatty acids (FFA) and cholesteryl ester (CE) analysis, total lipid fraction was separated by 1D-HPTLC using hexane/diethyl ether/formic acid, 80:20:2 (v/v/v) as solvent system. All lipid classes were identified by comparison of migration with authentic chemical standards. Thereafter, each lipid spot on the HPTLC plate was scrapped off and lipids were methanolized with 200 μL 0.5 M methanolic HCl in the presence of 1 nmol pentadecanoic acid (C15:0) as internal standard at 85°C for 3 h. The resulting FAMEs were extracted with hexane and finally analyzed by GC-MS (Agilent).

All analyses were performed in triplicate or more ($n = 3$ or $n = 6$). The p values of ≤ 0.05 from statistical analyses (Student's *t*-test) obtained from GraphPad software analysis were considered statistically significant.

To assess effect of drug treatment on lipidomic profiles, the parasites cultures were treated with selected drug compound at concentration $\sim EC_{50}$, followed by lipid extraction and analysis as described above.

Phospholipid uptake and flux analysis

Synchronous transgenic parasites in the *Pf*LPL3-iKD set and control set were grown in presence of fluorescent labeled lipid lysoPC12:0 (20μM). The labeled lysoPC12:0 contains NBD label on the fatty-acids [1-{12-[(7-nitro-2-1,3-benzoxadiazol-4-yl)amino]dodecanoyl}-2-hydroxy-sn-glycero-3-phosphocholine (Avanti Polar Lipids, Inc). Similarly, for drug assays synchronous *P. falciparum* 3D7 parasites were grown in presence of *Pf*LPL3 inhibitor (PCB6 or PCB7; at EC_{50} concentration) or solvent alone and then treated with of fluorescent labeled lipid lysoPC12:0 (20μM) at 32hpi. The levels of fluorescence label in parasites were assessed at 36hpi by fluorescence microscopy and flow cytometry. Flow cytometric analysis was carried out using the BD FACS Calibur system (Beckton Dickinson). Arbitrary fluorescence units for 100,000 cells were acquired on channels FL1 (FITC) using Cell Quest Pro (Beckton Dickinson) and data were analyzed using Graph Pad Prism v 5.0. Uninfected RBCs were used as background control.

Cloning, expression and purification of recombinant protein

Hydrolase domain of *Pf*LPL3 was amplified by using specific primers 1270A and 1271A (Table S1) and cloned in to pETM41 vector between *Nco*I and *Xho*I sites to give pETM41-His6-MBP-PfLPL3 construct. The recombinant protein *Pf*LPL3 was expressed as soluble protein in the cytosol of the *E. coli* BL21(DE3) codon$^+$ cells. For expression, bacterial cells having pETM41-His6-MBP-PfLPL3 was grown in of LB medium supplemented with kanamycin at 37°C to an absorbance (A_{600}) of ~0.8–1.0. Expression of the fusion proteins was induced using 1mM isopropyl β-D-thiogalactoside (IPTG) overnight at 16°C. Next day cells were harvested and resuspended into resuspension buffer (25mM Tris, pH7.4, 500mM NaCl, 10mM Imidazole) and lysed by sonication (Vibra cell sonicator). The supernatant was subjected a combination of Ni-NTA affinity chromatography followed by amylose affinity chromatography. Eluted fractions were subjected to SDS PAGE and Western blot analysis to assess the purity of the purified recombinant protein.

Lysophospholipase (LPL) activity assay and enzyme kinetics

For assessing the enzymatic activity of the recombinant *Pf*LPL3, a lysophospholipase (LPL) activity assay was established using lysophosphatidylcholine as substrate as described earlier.[33] Briefly, the activity assay reaction mixture (200 μL total volume) contained 16:0 lysophosphatidylcholine (LPC) as substrate, 20μg (285pmol) of recombinant protein, 0.1 unit glycerophosphodiesterase (Sigma), 0.2 U/ml choline oxidase (Sigma 26978), 2U/ml horseradish peroxidase (Sigma P8125), 100μM Amplex Red (Invitrogen) in a reaction buffer (50mM Tris pH 8.0, 5mM $CaCl_2$). The *Pf*LPL3 cleaves the acyl chain from LPC resulting the generation of glycerophosphocholine on which glycerophosphodiesterase acts and cleaves the choline moiety. This choline was oxidized by choline oxidase to produce betaine and H_2O_2. Finally, H_2O_2 in presence of horseradish peroxidase, reacts with Amplex Red reagent in 1:1 stoichiometry to generate the highly fluorescent product resorufin, which has absorption and fluorescence emission maxima of approximately 571 nM and 585 nM respectively. The LPL activity was monitored by measuring fluorescence intensities (530 ex/590 em) for 6 h using spectramax M2 microplate reader. The assay was performed by varying the amount of protein and substrate to get optimum LPL activity. The kinetic constant *K*m and *V*max were determined by fitting Michalies-Menten curve using the Graph Pad Prism V5.0 software package.

Standardization of a robust lysophospholipase (LPL) activity assay and screening of compound library

Robustness of the activity assays was assessed by conducting HML test for a period of two days in accordance for statistical test to calculate the Z-value. The HML assay employed three different reaction wells: **H**igh activity well i.e. lysophospholipase activity well with 20μg enzyme; **M**edium activity well i.e. in the presence reduced amount of enzyme, (10μg protein); and the **L**ow activity well that is the substrate control well without the enzyme; this set of three wells (HML) was repeated throughout the 96-well plate and the assay was repeated for two consecutive days. The Z-value was calculated based on the variations in activity between the wells/plates.[41]

To identify the *Pf*LPL3 targeting antimalarial compounds, ''Malaria Box'' compound library obtained from Medicines for Malaria Venture (MMV, Switzerland), was screened using the standardized *Pf*LPL3 activity assay; briefly, the recombinant enzyme (20μg) was incubated with different concentrations of each of the compound or DMSO alone; the reactions were initiated by addition of the activity assay reaction mixture to a final volume of 200μL and the substrate hydrolysis was monitored as described above. To assess the effect of selected *Pf*LPL3 inhibitors on parasite growth and morphology, synchronized parasite cultures at 1% ring stage parasites were treated with varied concentrations of each of the selected compounds (5.0–0.2μM), parasite growth was estimated in next cycle by flow cytometry. DMSO was used as a control.

QUANTIFICATION AND STATISTICAL ANALYSIS

The datasets were analyzed using GraphPad Prism ver 5.0 to calculate *K*m, *V*max, IC_{50} and EC_{50} values, and the data were compared using unpaired Student's *t*-test.